Low frequency graphene resonators for acoustic sensing

Citation for published version:
Grady, E, Mastropaolo, E, Chen, T, Bunting, A & Cheung, R 2014, 'Low frequency graphene resonators for acoustic sensing' Microelectronic Engineering, vol. 119, pp. 105-108. DOI: 10.1016/j.mee.2014.02.036

Digital Object Identifier (DOI):
10.1016/j.mee.2014.02.036

Link:
Link to publication record in Edinburgh Research Explorer

Document Version:
Peer reviewed version

Published In:
Microelectronic Engineering

Low frequency graphene resonators for acoustic sensing

Eldad Grady[1,*], Enrico Mastropaolo, Tao Chen, Andrew Bunting,
Rebecca Cheung

Scottish Microelectronics Centre, The University of Edinburgh, King's Buildings, Mayfield Road, Edinburgh EH9 3JF, Scotland, UK

Abstract

Graphene resonators have been fabricated in rectangular and circular geometries ranging from 1 to 3 mm in diameter. The resonant frequencies have been measured, and fitted to an analytical model. An optical profile of the graphene sheet has been taken, and the monolayer graphene has been confirmed to be of high quality using Raman spectroscopy. The graphene membranes have shown hookean behaviour with no evidence of deformation. The characterisation of the single layer graphene sheet on this large scale provides new information previously unavailable on the mechanical stability of graphene with ultra high aspect ratio.

Keywords: Graphene, Raman, Young's modulus, resonant frequency, acoustic sensing, MEMS

1. Introduction

The quest after an implant that mimics the functionalities of the cochlea, the hearing organ, has driven many researchers to seek for a suitable micro electromechanical systems (MEMS) device [1]. The use of MEMS for medical applications has allowed researchers to develop bionic substitutes for human sensory and functional deficits such as an artificial cochlea [2]. The miniaturization and optimization in terms of selectivity and robustness of the devices are the main focus of much research [3]. Sensing of acoustic waves can be done by transducing mechanical vibrations to electrical signals using a micro-sized bridge resonating at the audible frequencies. The displacement caused by the bridge resonance changes the capacitance between the beam-like bridge and the transistor channel underneath it, forming a Resonant gate transistor (RGT)[4]. Since the transistor's threshold voltage increases in proportion to the airgap, it is critical for the RGT bridge to retain a predictable and constant airgap over

---

[*] Corresponding author
Email address: `e.grady@ed.ac.uk` (Eldad Grady)
[1] Telephone: +44 (0)131 650623/ +44 (0)131 6507474

the transistor channel for a controlled and efficient operation. Therefore, a high in plane stiffness is crucial for achieving a constant airgap, in addition to a high Young's modulus necessary for structural stability of resonators designated for the lower frequency regime. A material that could answer these two essential demands could be a promising candidate for a highly efficient, low threshold voltage and sensitive RGT.

The introduction of graphene by Novoselov et al. [5] in 2004, opened new possibilities for faster, smaller electronic devices as well as ultra sensitive sensors due to the remarkable electrical and mechanical characteristics of graphene [6, 7]. An atom thick layer of graphene sheet exhibits exceptionally high Young's Modulus of 1 TPa, in-plane stiffness of 340 N/m and 42 N/m breaking strength [8], making it a promising candidate for ultra sensitive, low power acoustic sensor. Previous work has been focused on graphene resonators for high frequencies [9]. an array of micro-resonators has been fabricated by van der Zande et al. [10] by transfer of Chemical Vapor Deposition (CVD) grown graphene. They have demonstrated the feasibility of using CVD grown Single Layer Graphene (SLG) to produce large arrays of resonators with similar electrical and mechanical qualities as exfoliated graphene. These resonators varied in range between 1-30 µm, and showed conformity with the thin membrane under tension model of resonance. Graphene has also been used as an acoustic sound source [11]. Recently, a group from Berkeley has fabricated graphene speaker using an electrostatically driven circular multilayer graphene (MLG), 7 mm in diameter [12]. The MLG graphene has been electrically bias with DC voltage and suspended between two electrodes driving opposite AC voltage. The speaker has been able to emit sound within audible frequencies (20-20KHz) with outstanding frequency response and power efficiency. The focus of this paper is the development of graphene based resonators for acoustic sensing. In this work, the feasibility and characteristics of graphene as a resonator for the low frequency regime are explored.

2. Material and methods

One major limitation in the fabrication of graphene resonators is the control of size of graphene foils due to the exfoliation process of production. Developments in CVD growth techniques allow now for centimeter scale monolayer graphene sheets to be fabricated and synthesized in MEMS applications [13]. Figure 1 portrays the fabrication process of the graphene resonators. A layer of 1 µm thick silicon oxide has been grown thermally on silicon wafer to establish isolation between the silicon substrate and the overlaying graphene sheet. The substrate has been patterned by photolithographic techniques with Circular and rectangular trenches. The exposed SiO_2 layer on the wafer has been etched with Reactive Ion Etching (RIE) to the depth of 1 µm. Consequently, the wafer has been diced with a milling machine.

In order to prepare the graphene for manual transfer, the CVD grown graphene on copper foil was coated with 500 nm of PMMA as intermediate layer for physical support. The backside monolayer graphene of the double sided graphene on copper foil has been etched using oxygen plasma dry etching.

The now exposed copper foil has been etched using Ferrite Chloride (FeCl) for ˜30 minutes, by carefully placing the foils on the surface with the copper layer downwards. The PMMA-graphene membranes have been scooped using SiO_2 on silicon diced chips. After rinsing the PMMA coated graphene membrane in Deionised water, the graphene has been transferred manually to the chip substrate with the pre-patterned trenches. The chip has been left to dry for ˜1 day, to achieve good adhesion of the graphene to the substrate. Thereafter annealing at 330° Celsius has taken place, in order to remove the PMMA layer. No solvents have been used to remove the PMMA, as they interact with the graphene and damage it [14]. This method yields high quality graphene over trenches, which form the doubly clamped resonators.

By avoiding fabrication steps after the graphene transfer, the advantages of pristine graphene are kept.

3. Results

An optical micrograph image has been taken to establish the placement and cover of the graphene sheet over the trenches. The graphene sheet is clearly visible to the naked eye due to the difference in the refractive index between SiO_2 and graphene. With the aid of the micrograph, it is possible to achieve first assessment of yield and discover large tears in the transferred graphene membrane. Figure 3a shows an array of rectangular trenches covered fully with SLG. The borders of the graphene sheet on the SiO_2 layer are clearly visible.

Scanning electron microscope (SEM) imaging of the resonators gives an improved visualisation of the graphene over trench, and tears can be detected easily. As can be seen in figure 3b, a 2 mm x 2 mm squared trench fully covered with graphene sheet with no distinguishable ruptures.

Raman spectra has been taken to determine the quality of the suspended graphene sheets. Band structure shows a 2D band at 2695 cm^{-1}, a G band at 1585 cm^{-1} and D band at 1345 cm^{-1} [see figure 2b]. The 2D band has a sharp symmetric peak and can be well fitted with a Lorentzian, proving the graphene sheet to be single layer. The ratio between the 2D band and the G band is 2.7 indicates the high quality of the SLG. The D band peak is significantly lower in intensity from the G band suggesting very little defects in the graphene. Additionally, a mapping scan of the suspended graphene membrane has been taken across the trench and plotted together in a 3D figure [see figure 2a]. The 3D plot provides an overview of the band structure of a large area, determined by the chosen length of the scan and steps.

An optical profile of the membrane has been taken using Zygo's Interferometer. In order to achieve a 3D profile of the graphene resonator over the trench, a series of scans have been taken and stitched together. This produces important information on the topographical structure of the SLG over trench. Figure 4b shows the profile of a 2.4 mm long sheet of SLG with 200 nm sagging at the maximum displacement point at the centre of the sheet, leaving over 800 nm airgap above the bottom of the trench. Data of the graphene sagging over trench depths in relation to the trench's length has been plotted [see figure 4a].

Microelectronic Engineering, Volume 119, 2014, Pages 105–108, DOI: 10.1016/j.mee.2014.02.036

The SLG shows high stiffness and retains an overall constant displacement to length ratio. However, the ratio varies from chip to chip, due to difference in seamlessness of the SLG. Graphene sheets with evident ruptures have shown to have a higher sagging ratio. This ratio is important for the prediction of minimum required trench depth correlating to the length of the largest resonator. It also gives information on the strain of the membrane, which varies the resonant frequency significantly.

The resonance frequency of the resonators have been measured using a Laser Doppler Vibrometer (LDV) by actuating a piezoelectric disc with a pure sinusoidal signal. Fundamental resonant frequencies have been detected at 15.8-17 KHz for several 2.8 mm long membrane over trench at the centre of each graphene sheet. Although there are many analytical models for the vibrations of SLG Ávila et al. [15], Chen et al reported a good match for the membrane under tension model [16], with variations dependent on strain

$$f_{rectangular} = \frac{1}{2L}\sqrt{\frac{E\varepsilon}{\rho}} \qquad (1)$$

where L is the membrane's length, E is the Young's Modulus, ε is the strain and ρ is the 2-Dimensional mass density.

The resonant frequency can vary by two orders of magnitude for the same device size due to the strain of the graphene sheet. This dependence, along with the reported breaking strain of 25%, means highly tunable resonators surpassing any other thin membrane resonators currently known. The measured fundamental resonant frequencies match the analytical model of doubly clamped rectangular membrane with 0.001% strain. The predicted 12 KHz resonant frequency by this simple model is well within the measured 1st mode peaks [see figure 5a].

4. Conclusions

Single layer graphene sheets have shown to be mechanically stable with ultra high aspect ratio. The profiling of SLG in this scale provides new information, previously unavailable. The membranes have exhibited very little sagging, about 0.01%, due to their high stiffness, meaning the linear elasticity model is valid for graphene with ultra high aspect ratio. Furthermore, graphene sheets integrated as gates of RGTs could achieve a lower operating voltage by the notably smaller airgap over the channel. Due to the reducedairgap, even small amplitude vibrations can actuate the transistor, which can increase the sensor's sensitivity. The device's design has a planar profile with no protruding objects over the surface, thus expected to be more robust and reliable than previous designs. The extraordinary properties of graphene are kept since no fabrication steps have taken place after graphene transfer, and due to the dry PMMA removal steps. The resonance of the SLG over trench can be fitted well with simple thin membrane model, with size and strain dependencies. High resonant frequency tunability promises good selectivity and wide operation range for future devices.

Acknowledgements

The authors would like to thank John Hedley and Zhongxu Hu for assistance with the LDV measurements, Andrei Gromov and Oleg Nerushev for help with Raman spectroscopy.

[1] T. Hamilton, C. Jin, A. van Schaik, J. Tapson, Biomedical Circuits and Systems, IEEE Transactions on 2 (2008) 30 –43. doi:10.1109/TBCAS.2008.921602.

[2] M. Bachman, F. Zeng, T. Xu, G. Li, Audiology and Neurotology 11 (2006) 95–103.

[3] A. GRAYSON, R. SHAWGO, A. JOHNSON, N. FLYNN, Y. LI, M. CIMA, R. LANGER, Proceedings of the IEEE 92 (2004) 6 – 21. doi:10.1109/JPROC.2003.820534.

[4] R. Latif, E. Mastropaolo, A. Bunting, R. Cheung, T. Koickal, A. Hamilton, M. Newton, L. Smith, Journal of Vacuum Science Technology B: Microelectronics and Nanometer Structures 29 (2011) 06FE05 –06FE05–6. doi:10.1116/1.3662408.

[5] K. Novoselov, A. Geim, S. Morozov, D. Jiang, Y. Zhang, S. Dubonos, I. Grigorieva, A. Firsov, Science 306 (2004) 666–669.

[6] A. Geim, K. Novoselov, Nature materials 6 (2007) 183–191.

[7] D. R. Cooper, B. D'Anjou, N. Ghattamaneni, B. Harack, M. Hilke, A. Horth, N. Majlis, M. Massicotte, L. Vandsburger, E. Whiteway, V. Yu, ArXiv e-prints (2011).

[8] C. Chen, J. Hone, Proceedings of the IEEE 101 (2013) 1766–1779. doi:10.1109/JPROC.2013.2253291.

[9] S. Gupta, R. Batra, Journal of Computational and Theoretical Nanoscience 7 (2010) 2151–2164. doi:doi:10.1166/jctn.2010.1598.

[10] A. van der Zande, R. Barton, J. Alden, C. Ruiz-Vargas, W. Whitney, P. Pham, J. Park, J. Parpia, H. Craighead, P. McEuen, Nano Lett 10 (2010) 4869–4873.

[11] J. W. Suk, K. Kirk, Y. Hao, N. A. Hall, R. S. Ruoff, Advanced Materials 24 (2012) 6342–6347. doi:10.1002/adma.201201782.

[12] Q. Zhou, A. Zettl, Applied Physics Letters 102 (2013) –. doi:http://dx.doi.org/10.1063/1.4806974.

[13] Y. Lee, S. Bae, H. Jang, S. Jang, S. Zhu, S. Sim, Y. Song, B. Hong, J. Ahn, Nano letters 10 (2010) 490–493.

[14] Y.-C. Lin, C.-C. Lu, C.-H. Yeh, C. Jin, K. Suenaga, P.-W. Chiu, Nano Letters 12 (2012) 414–419. doi:10.1021/nl203733r.

[15] A. F. Ávila, A. C. Eduardo, A. S. Neto, Comput. Struct. 89 (2011) 878–892. doi:10.1016/j.compstruc.2011.02.017.

[16] C. Chen, Graphene NanoElectroMechanical Resonators and Oscillators, Ph.D. thesis, Columbia University, 2013.

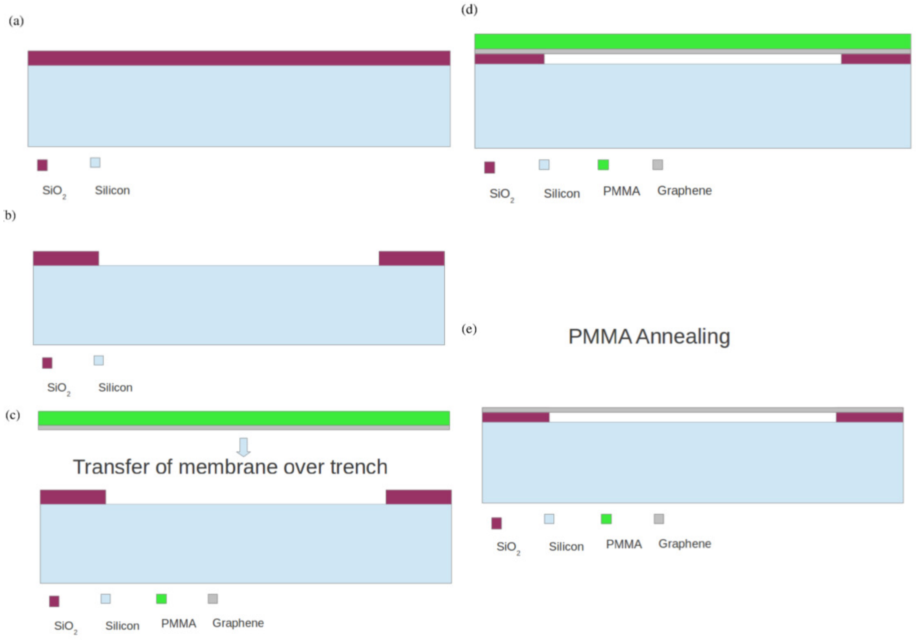

Figure 1: Fabrication steps; (a) thermal deposition of oxide. (b) lithography steps. patterning of trenches. (c) etching copper foil and transfer of PMMA coated graphene. (d) membrane left to dry for stronger adhesion to substrate. e) PMMA layer annealed at 330° Celsius.

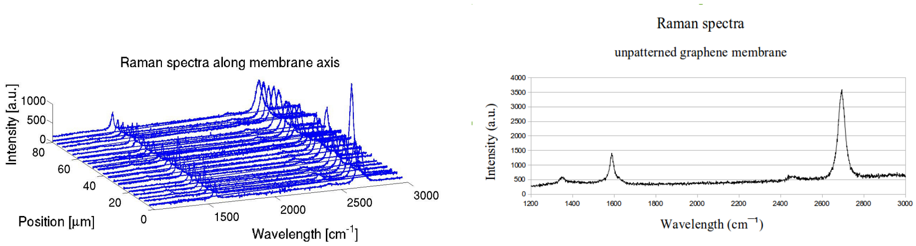

(a) (b)

Figure 2: (a) 3D Raman spectra of suspended monolayer graphene. Band structure is plotted across the length of the membrane with constant steps of scanning. (b) Raman spectra of the membrane after annealing the PMMA. The 2D band at 2700 cm^{-1} indicates it is a single layer graphene sheet.

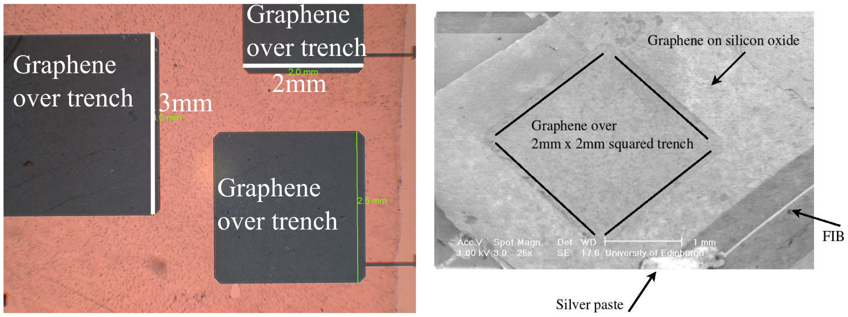

(a) (b)

Figure 3: (a) Optical micrograph image of rectangular resonators array. (b) SEM image of a rectangular graphene membrane over trench with a 2 mm diameter.

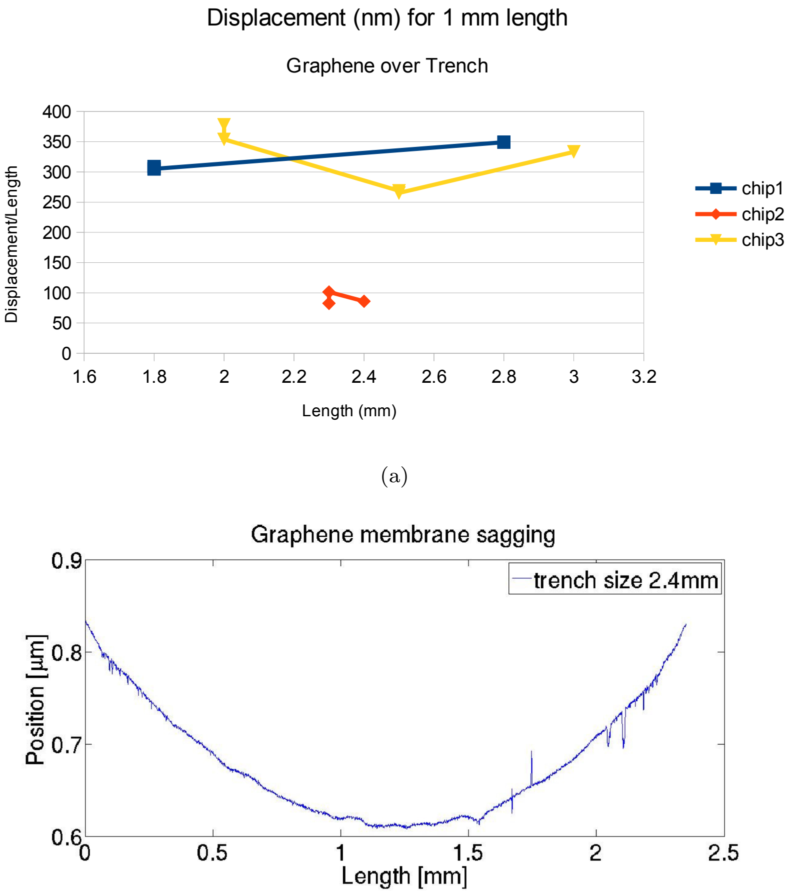

(a)

(b)

Figure 4: (a) Displacement to length ratio of sagging for SLG sheet. Sagging varies between chips but ratio is approximately constant for each chip. (b) Curvature of SLG sheet optically profiled using an interferometer.

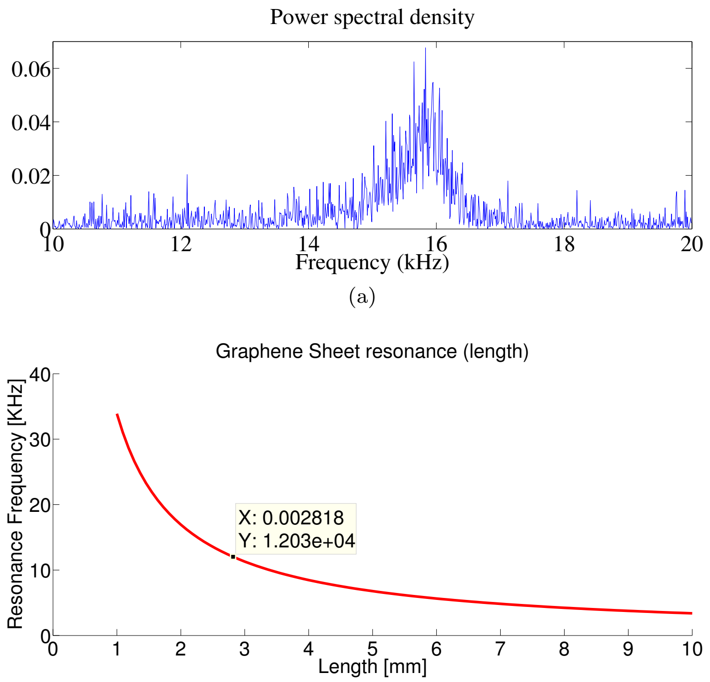

(a)

(b)

Figure 5: (a) Measured resonance frequency for 2.8 mm long membrane using LDV. (b) Analytical model of SLG resonance. The SLG is modeled as a simple rectangular thin-membrane under tension. The model predicts resonance of the graphene sheet at 12 KHz for 2.82 mm long sheet.